(Non)existence of Pleated Folds:
How Paper Folds Between Creases

Erik D. Demaine*†   Martin L. Demaine*   Vi Hart‡

Gregory N. Price*   Tomohiro Tachi§

Abstract

We prove that the pleated hyperbolic paraboloid, a familiar origami model known since 1927, in fact cannot be folded with the standard crease pattern in the standard mathematical model of zero-thickness paper. In contrast, we show that the model can be folded with additional creases, suggesting that real paper "folds" into this model via small such creases. We conjecture that the circular version of this model, consisting simply of concentric circular creases, also folds without extra creases.

At the heart of our results is a new structural theorem characterizing uncreased intrinsically flat surfaces—the portions of paper between the creases. Differential geometry has much to say about the local behavior of such surfaces when they are sufficiently smooth, e.g., that they are torsal ruled. But this classic result is simply false in the context of the whole surface. Our structural characterization tells the whole story, and even applies to surfaces with discontinuities in the second derivative. We use our theorem to prove fundamental properties about how paper folds, for example, that straight creases on the piece of paper must remain piecewise-straight (polygonal) by folding.

1   Introduction

A fascinating family of *pleated* origami models use extremely simple crease patterns—repeated concentric shapes, alternating mountain and valley—yet automatically fold into interesting 3D shapes. The most well-known is the *pleated hyperbolic paraboloid*, shown in Figure 1, where the crease pattern is concentric squares and their diagonals. As the name suggests, it has long been conjectured, but never formally established, that this model approximates a hyperbolic paraboloid. More impressive (but somewhat harder to fold) is the *circular pleat*, shown in Figure 2, where the crease pattern is simply concentric circles, with a circular hole cut out of the center. Both of these models date back to the Bauhaus, from a preliminary course in paper study taught by Josef Albers in 1927–1928 [Win69, p. 434], and taught again later at Black Mountain College in 1937–1938 [Adl04, pp. 33, 73]; see [DD08]. These models owe their popularity today to origamist Thoki Yenn, who started distributing the model sometime before 1989. Examples of their use and extension for algorithmic sculpture include [DDL99, KDD08].

---

*MIT Computer Science and Artificial Intelligence Laboratory, 32 Vassar St., Cambridge, MA 02139, USA, {edemaine,mdemaine,price}@mit.edu.
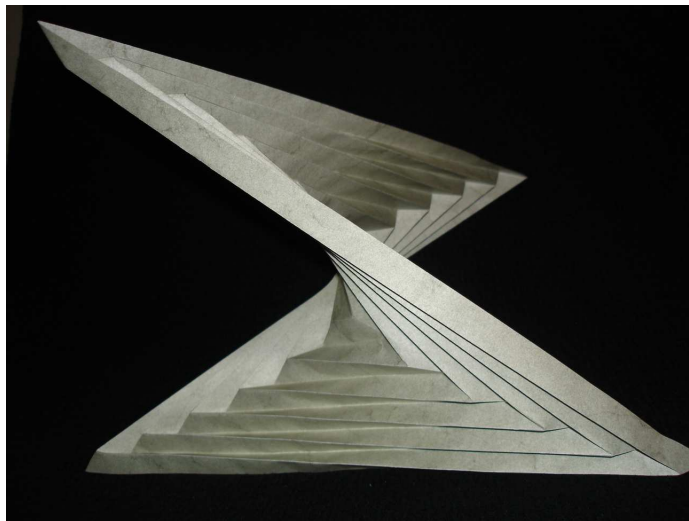
†Partially supported by NSF CAREER award CCF-0347776.

‡http://vihart.com

§Department of Architecture, The University of Tokyo, 7-3-1 Hongo, Bunkyo, Tokyo 113-8658, Japan, ttachi@siggraph.org
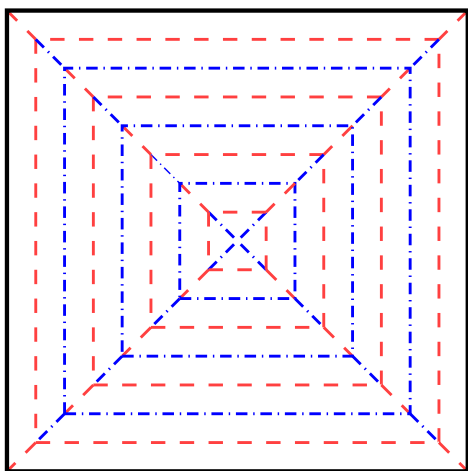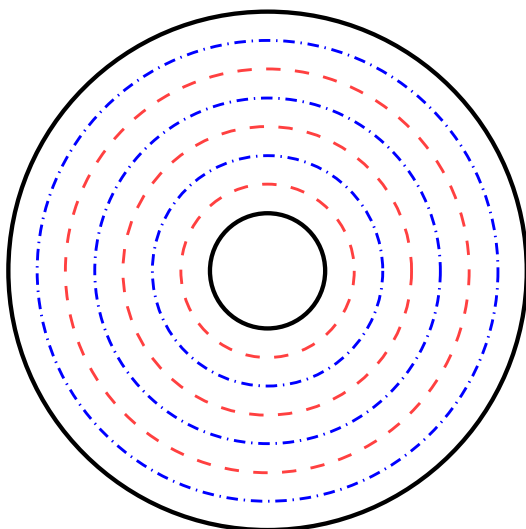
(a) Standard mountain-valley pattern.   (b) Photograph of physical model. [Jenna Fizel]

Figure 1: Pleated hyperbolic paraboloid.

(a) Mountain-valley pattern.   (b) Photograph of physical model. [Jenna Fizel]

Figure 2: Circular pleat.

The magic of these models is that most of the actual folding happens by the physics of paper itself; the origamist simply puts all the creases in and lets go. Paper is normally elastic: try wrapping a paper sheet around a cylinder, and then letting go—it returns to its original state. But *creases* plastically deform the paper beyond its yield point, effectively resetting the elastic memory of paper to a nonzero angle. Try creasing a paper sheet and then letting go—it stays folded at the crease. The harder you press the crease, the larger the desired fold angle. What happens in the pleated origami models is that the paper tries to stay flat in the uncreased portions, while trying to stay folded at the creases, and physics computes a configuration that balances these forces in equilibrium (with locally minimum free energy).

But some mathematical origamists have wondered over the years [Wer05]: do these models actually *exist*? Is it really possible to fold a piece of paper along exactly the creases in the crease pattern of Figures 1 and 2? The first two authors have always suspected that both models existed, or at least that one existed if and only if the other did. But we were wrong.

Our results. We prove that the hyperbolic-paraboloid crease pattern of Figure 1(a) does not fold using exactly the given creases, even with a hole cut out of the center.

In proving the impossibility of folding the pleated hyperbolic paraboloid, we develop a structural characterization of how uncreased paper can fold (hence the title of this paper). Surprisingly, such a characterization has not been obtained before. An intuitive understanding (often misquoted) is that paper folds like a ruled surface, but that claim is only true locally (infinitesimally) about every point. When the paper is not smooth or has zero principal curvature at some points, the truth gets even subtler. We correct both of these misunderstandings by handling nonsmooth (but uncreased) surfaces, and by stating a local structure theorem flexible enough to handle zero curvatures and all other edge cases of uncreased surfaces.

In contrast, we conjecture that the circular-pleat crease pattern of Figure 2(a) folds using exactly the given creases, when there is a hole cut out of the center. A proof of this would be the first proof of existence of a curved-crease origami model (with more than one crease) of which we are aware. Existing work characterizes the local folding behavior in a narrow strip around a curved crease, and the challenge is to extend this local study to a globally consistent folding of the entire crease pattern.

Another natural remaining question is what actually happens to a real pleated hyperbolic paraboloid like Figure 1(b). One conjecture is that the paper uses extra creases (discontinuities in the first derivative), possibly many very small ones. We prove that, indeed, simply triangulating the crease pattern, and replacing the four central triangles with just two triangles, results in a foldable crease pattern. Our proof of this result is quite different in character, in that it is purely computational instead of analytical. We use interval arithmetic to establish with certainty that the exact object exists for many parameter values, and its coordinates could even be expressed by radical expressions in principle, but we are able only to compute arbitrarily close approximations.

2 Structure of Uncreased Flat Surfaces

Our impossibility result rests on an understanding of how it is possible to fold the faces of the crease pattern, which by definition are regions folded without creases. The geometric crux of the proof therefore relies on a study of uncreased intrinsically flat (paper) surfaces. This section gives a detailed analysis of such surfaces. Our analysis allows discontinuities all the way down to the second derivative (but not the first derivative—those are creases), provided those discontinuities are somewhat tame.

We begin with some definitions, in particular to nail down the notion of creases.

Definition 1 *For us a* surface *is a compact 2-manifold embedded in $\mathbb{R}^3$. The surface is C^k if the manifold and its embedding are C^k. The surface is* piecewise-C^k *if it can be decomposed as a complex of C^k regions joined by vertices and C^k edges.*

Definition 2 *A* good surface *is a piecewise-C^2 surface. A good surface S therefore decomposes into a union of C^2 surfaces S_i, called* pieces, *which share C^2 edges γ_j, called* semicreases, *whose endpoints are* semivertices. *Isolated points of C^2 discontinuities are also* semivertices. *If S is itself*

C^1 *everywhere on a semicrease, we call it a* proper semicrease; *otherwise it is a* crease. *Similarly a semivertex v is a* vertex *if S is not C^1 at v. Accordingly an* uncreased surface *is a C^1 good surface (with no creases or vertices), and a* creased surface *is a good surface not everywhere C^1 (with at least one crease or vertex).*

Definition 3 *A surface is* (intrinsically) flat *if every point p has a neighborhood isometric to a region in the plane.*[1]

In order to understand the uncreased flat surfaces that are our chief concern, we study the C^2 flat surfaces that make them up. On a C^2 surface, the well-known *principal curvatures* $\kappa_1 \geq \kappa_2$ are defined for each interior point as the maximum and minimum (signed) curvatures for geodesics through the point. A consequence of Gauss's celebrated Theorema Egregium [Gau02] is that, on a C^2 flat surface, the *Gaussian curvature* $\kappa_1\kappa_2$ must be everywhere zero. Thus every interior point of a C^2 flat surface is either *parabolic* with $k_2 \neq k_1 = 0$ or *planar* with $k_2 = k_1 = 0$.

Each interior point p on a C^2 flat surface therefore either

   (a) is planar, with a planar neighborhood;

   (b) is planar and the limit of parabolic points; or

   (c) is parabolic, and has a parabolic neighborhood by continuity,

and an interior point on an uncreased flat surface may additionally

   (d) lie on the interior of a semicrease; or

   (e) (a priori) be a semivertex.

For points of type (a), it follows by integration that the neighborhood has a constant tangent plane and indeed lies in this plane. Types (b) and (c) are a bit more work to classify, but the necessary facts are set forth by Spivak [Spi79, vol. 3, chap. 5, pp. 349–362] and recounted below. (In Spivak's treatment the regularity condition is left unspecified, but the proofs go through assuming only C^2.) We address type (d) farther below. From our results it will become clear that the hypothetical type (e) does not occur in uncreased flat surfaces.

Proposition 1 [Spi79, Proposition III.5.4 et seq.] *For every point p of type (c) on a surface M, a neighborhood $U \subset M$ of p may be parametrized as*

$$f(s,t) = c(s) + t \cdot \delta(s)$$

where c and δ are C^1 functions; $c(0) = p$; $|\delta(s)| = 1$; $c'(s)$, $\delta(s)$, and $\delta'(s)$ are coplanar for all s; and every point of U is parabolic.

Write interior(M) for the interior of a surface M.

Proposition 2 [Spi79, Corollaries III.5.6–7] *For every point p of type (b) or (c) on a surface M, there is a unique line L_p passing through p such that the intersection $L_p \cap M$ is open in L_p at p. The component C_p containing p of the intersection $L_p \cap$ interior(M) is an open segment, and every point in C_p is also of type (b) or (c) respectively.*

---

[1]Henceforth we use the term "flat" for this intrinsic notion of the surface metric, and the term "planar" for the extrinsic notion of (at least locally) lying in a 3D plane.

Following the literature on flat surfaces, we speak of a segment like the C_p of Proposition 2 as a *rule segment*. The *ruling* of a surface is the family of rule segments of all surface points, whose union equal the surface. A ruling is *torsal* if all points along each rule segment have a common tangent plane.

To characterize points of type (d), lying on semicreases, we require the following two propositions.

Proposition 3 *Consider a point q of type (d) on a surface M. Then q is not the endpoint of the rule segment C_p for any point $p \in M$ of type (b) or (c).*

Proof: It suffices to show the conclusion for p of type (c), because a rule segment of type (b) is a limit of rule segments of type (c). Let γ be the interior of the semicrease on which q lies.

Because M is C^1, it has a tangent plane M_q at each q, which is common to the two C^2 pieces bounded by γ. Parametrize γ by arclength with $\gamma(0) = q$, and write $n(s)$ for the unit normal to the tangent plane $M_{\gamma(s)}$. Parametrize the two pieces as torsal ruled surfaces by the common curve $c_1(s) = c_2(s) = \gamma(s)$ and lines $\delta_1(s)$ and $\delta_2(s)$. Then, because each piece is torsal, $\dot{n}(s) \perp \delta_1(s)$ and $\dot{n}(s) \perp \delta_2(s)$. But both $\delta_1(s)$ and $\delta_2(s)$ lie in the tangent plane at s, perpendicular to $n(s)$, and so too does $\dot{n}(s)$ because $n(s)$ is always a unit vector. Therefore, for each s, either $\dot{n}(s) = 0$ or $\delta_1(s)$ and $\delta_2(s)$ are collinear.

Let A be the subset of γ on which $\dot{n}(s) = 0$, and B the subset on which $\delta_1(s)$ and $\delta_2(s)$ are collinear. Then we have shown that $A \cup B = \gamma$. By continuity, both A and B are closed. Therefore any point of γ which does not belong to A is in the interior of B, and any point not in the interior of A is in the closure of the interior of B.

If an open interval I along γ is contained in A so that $\dot{n}(s) = 0$, then a neighborhood in M of I is planar by integration because each rule segment has a single common tangent plane in a torsal ruled surface. On the other hand if I is contained in B so that $\delta_1(s)$ and $\delta_2(s)$ are collinear, then a neighborhood is a single C^2 ruled surface. In either case, the rule segments from one surface that meet I continue into the other surface. That is, each rule segment meeting a point in the interior of A or B continues into the other surface.

Now we conclude. By continuity, each rule segment meeting a point in the closure of the interior of A or B continues into the other surface; but these two closures cover γ. So no rule segment ends on γ, including at q. □

Proposition 4 *For every point p of type (d) on a surface M, there is a unique line L_p passing through p such that the intersection $L_p \cap M$ is open in L_p at p. The component C_p containing p of the intersection $L_p \cap \mathrm{interior}(M)$ is an open segment, the limit of rule segments through points neighboring p, and every point of C_p is also of type (d).*

Proof: Let $B_r(p)$ be a radius-r disk in M centered at p, small enough that no point of the disk is a semivertex. By Proposition 3, the rule segment through any point q of type (b) or (c) in the half-size disk $B_{r/2}(p)$ cannot end in $B_r(p)$, so it must be of length at least $r/2$ in each direction. Further, p must be a limit of such points, or else a neighborhood of p would be planar.

By a simple compactness argument, provided in [Spi79] for the type-(b) case of Proposition 2, C_p is the limit of (a subsequence of) rule segments C_q through points q of type (b) and (c) approaching p and is an open segment. Because each C_q has a single tangent plane, the discontinuity in second derivatives found at p is shared along C_p. □

Two corollaries follow immediately from Proposition 4.

Corollary 5 *Every (proper) semicrease in an uncreased flat surface is a line segment, and its endpoints are boundary points of the surface.*

Corollary 6 *An uncreased flat surface has no interior semivertices; every interior point is in the interior of a C^2 piece or a semicrease.*

Another corollary summarizes much of Propositions 2 and 4 combined.

Corollary 7 *Every interior point p of an uncreased flat surface M not belonging to a planar neighborhood belongs to a unique rule segment C_p. The rule segment's endpoints are on the boundary of M, and every interior point of C_p is of the same type (b), (c), or (d).*

Finally, we unify the treatment of all types of points in the following structure theorem for uncreased flat surfaces. The theorem is similar to Proposition 1, which concerns only points of type (c).

Theorem 8 *Every interior point of an uncreased flat surface has a neighborhood that is a ruled surface. In each rule segment, every interior point is of the same type (a), (b), (c), or (d). The ruled surface may be parametrized as*

$$f(s,t) = c(s) + t \cdot \delta(s),$$

where c is C^1, δ is C^0, and δ is C^1 whenever $c(s)$ is of type (a), (b), or (c).

Proof: Let p be a point on an uncreased flat surface M. If p is of type (a), then we may parametrize its planar neighborhood as a ruled surface almost arbitrarily. Otherwise, p is of type (b), (c), or (d) and has a unique rule segment C_p.

Embed a neighborhood $U \subset M$ of C_p isometrically in the plane, by a map $\phi : U \to \mathbb{R}^2$. Let γ be a line segment in the plane perpendicularly bisecting $\phi(C_p)$, parametrized by arclength with $\gamma(0) = \phi(p)$. Every point $\phi^{-1}(\gamma(s))$ of type (b), (c), or (d) has a unique rule segment $C_{\phi^{-1}(\gamma(s))}$; for such s, let $\varepsilon(s)$ be the unit vector pointing along $\phi(C_{\phi^{-1}(\gamma(s))})$, picking a consistent orientation.

Now the remaining s are those for which $\phi^{-1}(\gamma(s))$ is of type (a). These s form an open subset, so that for each such s there is a previous and next s not of type (a). For each such s, we can determine an $\varepsilon(s)$ by interpolating angles linearly between the $\varepsilon(s)$ defined for the previous and next s not of type (a). The resulting function $\varepsilon(s)$ is continuous and identifies a segment through every point in γ, giving a parametrization of a neighborhood of γ as a ruled surface by $g(s,t) = \gamma(s) + t \cdot \varepsilon(s)$.

Finally, write $f(s,t) = \phi^{-1}(g(s,t))$ to complete the construction. □

3 How Polygonal Faces Fold

If all edges of the crease pattern are straight, every face of the crease pattern is a polygon. We first show that, if the edges of such a polygon remain straight (or even piecewise straight) in space, then the faces must remain planar.

Theorem 9 *If the boundary of an uncreased flat surface M is piecewise linear in space, then M lies in a plane.*

Proof: Let p be a parabolic point in the interior of M, a point of type (c). We will show a contradiction. It then follows that every point of M is of type (a), (b), or (d), so planar points of type (a) are dense and by integration M lies in a plane.

Because p is parabolic, it has by Proposition 1 a neighborhood consisting of parabolic points which is a ruled surface. By Corollary 7, the rule segment through each point in this neighborhood can be extended to the boundary of M. Let U be the neighborhood so extended.

Now the boundary of U consists of a first rule segment ab, a last rule segment cd, and arcs bd and ac of which at least one must be nontrivial, say bd. Because we extended U to the boundary of M and the boundary of M is piecewise linear, bd consists of a chain of segments. Let $b'd'$ be one of these segments.

Let q be any point interior to the segment $b'd'$, and consider the normal vector $n(q)$ to M at q. The normal is perpendicular to $b'd'$ and to the rule segment C_q meeting q. Because U is torsal, its derivative $n'(q)$ along $b'd'$ is also perpendicular to C_q, and because the normal is always perpendicular to $b'd'$ the derivative is perpendicular to $b'd'$. But this forces $n'(q)$ to be a multiple of $n(q)$, therefore zero, which makes the points of C_q planar and is a contradiction. $\qquad\square$

4   Straight Creases Stay Straight

Next we show that straight edges of a crease pattern must actually fold to straight line segments in space.

Theorem 10 *If γ is a geodesic crease in a creased flat surface M with fold angle distinct from $\pm 180°$, then γ is a segment in $\mathbb{R}^3$.*

Proof: The creased surface M decomposes by definition into a complex of uncreased surfaces, creases, and vertices. A point p in the interior of γ is therefore on the boundary of two uncreased pieces; call them S and T. Let S_p and T_p be the tangent planes to S and T respectively at p. Because γ is by hypothesis not a proper semicrease, has no semivertices along it, and has a fold angle distinct from $\pm 180°$, there is some $p \in \gamma$ where $S_p \neq T_p$. By continuity, the same is true for a neighborhood in γ of p; let U be the maximal such neighborhood.

Now parametrize γ by arclength and let $p = \gamma(s)$. At each $q = \gamma(t)$, the tangent vector $\gamma'(t)$ lies in the intersection $S_q \neq T_q$; in U, this determines $\gamma'(t)$ up to sign. Because S and T are C^2, the tangent planes S_q and T_q are C^1, hence so is $\gamma'(t)$, and the curvature $\gamma''(t)$ exists and is continuous.

Now around any $q \in U$ project γ onto the tangent plane S_q. Because γ is a geodesic, we get a curve of zero curvature at q, so $\gamma''(t)$ must be perpendicular to S_q. Similarly $\gamma''(t) \perp T_q$. But certainly $\gamma''(t) \perp \gamma'(t)$. So $\gamma''(t) = 0$.

We have $\gamma''(t) = 0$ for t in a neighborhood of s, so γ is a segment on U. Further, by the considerations of Theorem 9, the tangent planes S_q and T_q are constant on U. Therefore they remain distinct at the endpoints of U, and because U is maximal, these must be the endpoints of γ and γ is a segment. $\qquad\square$

Combining the previous two theorems, we deduce that polygonal faces of the crease pattern with no boundary edges must indeed stay planar:

Corollary 11 *If an uncreased region of a creased flat surface M is piecewise geodesic and entirely interior to M, then the region lies in a plane.*

5   Nonexistence of Pleated Hyperbolic Paraboloid

Now we can apply our theory to prove nonfoldability of crease patterns. First we need to formally define what this means.

Definition 4 *A* piece of paper *is a planar compact 2-manifold. A* crease pattern *is a graph embedded into a piece of paper, with each edge embedded as a non-self-intersecting curve. A* proper folding *of a crease pattern is an isometric embedding of the piece of paper into 3D whose image is a good surface such that the union of vertices and edges of the crease pattern map onto the union of vertices and creases of the good surface. A* rigid folding *is a proper folding that maps each face of the crease pattern into a plane (and thus acts as a rigid motion on each face).*

Note that a proper folding must fold every edge of the crease pattern by an angle distinct from 0 (to be a crease) and from $\pm 180°$ (to be an embedding). We call such fold angles *nontrivial*. Also, one edge of a crease pattern may map to multiple creases in 3D, because of intervening semivertices.

The key property we need from the theory developed in the previous sections is the following consequence of Corollary 11:

Corollary 12 *For any crease pattern made up of just straight edges, any proper folding must fold the interior faces rigidly.*

We start by observing that the center of the standard crease pattern for a pleated hyperbolic paraboloid has no proper folding.

Lemma 13 *Any crease pattern containing four right triangular faces, connected in a cycle along their short edges, has no rigid folding.*

Proof: This well-known lemma follows from, e.g., [DO02, Lemma 9]. For completeness, we give a proof. Let v_1, v_2, v_3, and v_4 denote the direction vectors of the four short edges of the triangular faces, in cyclic order. By the planarity of the faces, the angle between adjacent direction vectors is kept at $90°$. Thus the folding angle of edge i equals the angle between v_{i-1} and v_{i+1} (where indices are treated modulo 4). If edge 2 is folded nontrivially, then v_1 and v_3 are nonparallel and define a single plane Π. Because v_2 is perpendicular to both v_1 and v_3, v_2 is perpendicular to Π. Similarly, v_4 is perpendicular to Π. Thus v_2 and v_4 are parallel, and hence edge 3 is folded trivially. Therefore two consecutive creases cannot both be folded nontrivially.   □

Corollary 14 *The standard crease pattern for a pleated hyperbolic paraboloid (shown in Figure 1(a)), with $n \geq 2$ rings, has no proper folding.*

Proof: With $n \geq 2$ rings, the four central triangular faces are completely interior. By Corollary 12, any proper folding keeps these faces planar. But Lemma 13 forbids these faces from folding rigidly.   □

The standard crease pattern for a pleated hyperbolic paraboloid cannot fold properly for a deeper reason than the central ring. To prove this, we consider the *holey crease pattern* in which the central ring of triangles has been cut out, as shown in Figure 3(a). If there were n rings in the initial crease pattern (counting the central four triangles as one ring), then $n - 1$ rings remain.

Theorem 15 *The holey crease pattern for a pleated hyperbolic paraboloid (shown in Figure 3(a)), with $n - 1 \geq 3$ rings, has no proper folding.*

8
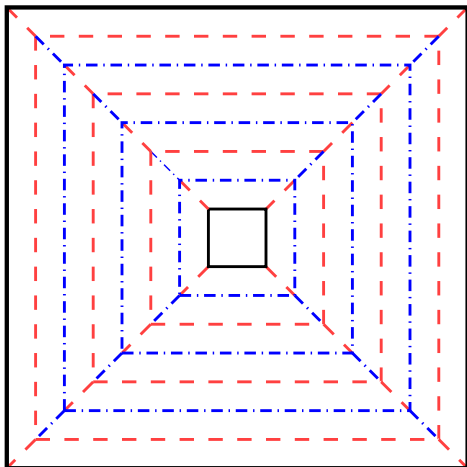
(a) Holey mountain-valley pattern for the pleated hyperbolic paraboloid.
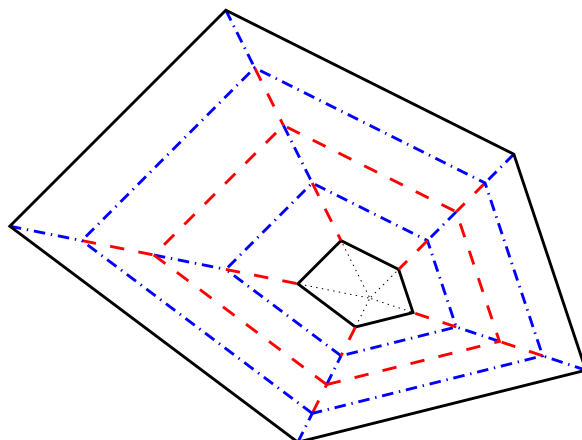
(b) Holey concentric pleat mountain-valley pattern.

Figure 3: Holey mountain-valley patterns which have no proper foldings.

Proof: Consider any nonboundary square ring of the crease pattern. By Corollary 12, the four trapezoidal faces each remain planar. Any folding of these four faces in fact induces a folding of their extension to four meeting right triangles. But Lemma 13 forbids these faces from folding rigidly. □

A different argument proves nonfoldability of a more general pleated crease pattern. Define the *concentric pleat crease pattern* to consist of n uniformly scaled copies of a convex polygon P, in perspective from an interior point p, together with the "diagonals" connecting p to each vertex of each copy of P. The outermost copy of the polygon P is the boundary of the piece of paper, and in the *holey concentric pleat mountain-valley pattern* we additionally cut out a hole bounded by the innermost copy of P. Thus $n - 1$ rings remain; Figure 3(b) shows an example.

First we need to argue about which creases can be mountains and valleys.

Definition 5 *A* mountain-valley pattern *is a crease pattern together with an assignment of signs (+1 for "mountain" and −1 for "valley") to the edges of a crease pattern. A* proper folding *of a mountain-valley pattern, in addition to being a proper folding of the crease pattern, must have the signs of the fold angles (relative to some canonical orientation of the top side of the piece of paper) match the signs of the mountain-valley assignment.*

Lemma 16 *A single-vertex mountain-valley pattern consisting of entirely mountains or entirely valleys has no proper rigid folding.*

Proof: If we intersect the piece of paper with a (small) unit sphere centered at the vertex, we obtain a spherical polygon whose edge lengths match the angles between consecutive edges of the crease pattern. (Here we rely on the fact that the vertex is intrinsically flat, so that the polygon lies in a hemisphere and thus no edges go the "wrong way" around the sphere.) The total perimeter of the spherical polygon is 360°. Any rigid folding induces a non-self-intersecting spherical polygon, with mountain folds mapping to convex angles and valley folds mapping to reflex angles, or vice versa (depending on the orientation of the piece of paper). To be entirely mountain or entirely valley, the folded spherical polygon must be locally convex, and by non-self-intersection, convex.

9

But any convex spherical polygon (that is not planar) has perimeter strictly less than 360° [Hal85, page 265, Theorem IV], a contradiction. □

Lemma 17 *Consider a rigidly foldable degree-4 single-vertex mountain-valley pattern with angles θ_1, θ_2, θ_3, and θ_4 in cyclic order. Then exactly one edge of the mountain-valley pattern has sign different from the other three, and if $\theta_2 + \theta_3 \geq 180°$, then the unique edge cannot be the one between θ_2 and θ_3.*

Proof: Again we intersect the piece of paper with a (small) unit sphere centered at the vertex to obtain a spherical polygon, with edge lengths θ_1, θ_2, θ_3, and θ_4, and whose convex angles correspond to mountain folds and whose reflex angles correspond to valley folds, or vice versa. By Lemma 16, at least one vertex is reflex, and thus the remaining vertices must be convex. (The only non-self-intersecting spherical polygons with only two convex vertices lie along a line, and hence have no reflex vertices. Here we rely on the fact that the vertex is intrinsically flat, so that the polygon lies in a hemisphere, to define the interior.) The two edges incident to this vertex form a triangle, by adding a closing edge. The other two edges of the quadrilateral also form a triangle, with the same closing edge, that strictly contains the previous triangle. The latter triangle therefore has strictly larger perimeter than the former triangle, as any convex spherical polygon has larger perimeter than that of any convex spherical polygon it contains [Hal85, page 264, Theorem III]. The two triangles share an edge which appears in both perimeter sums, so we obtain that the two edges incident to the reflex angle sum to less than half the total perimeter of the quadrilateral, which is 360°. Therefore they cannot be the edges corresponding to angles θ_2 and θ_3. □

Now we can prove the nonfoldability of a general concentric pleat:

Theorem 18 *The holey concentric pleat crease pattern (shown in Figure 3(b)), with $n - 1 \geq 4$ rings, has no proper folding.*

Proof: First we focus on two consecutive nonboundary rings of the crease pattern, which by Corollary 12 fold rigidly. Each degree-4 vertex between the two rings has a consecutive pair of angles summing to more than 180° (the local exterior of P), and two consecutive pairs of angles summing to exactly 180° (because the diagonals are collinear). By Lemma 17, the interior diagonal must be the unique crease with sign different from the other three. Thus all of the creases between the rings have the same sign, which is the same sign as all of the diagonal creases in the outer ring.

Now focus on the outer ring, whose diagonal creases all have the same sign. Any folding of the faces of a ring in fact induces a folding of their extension to meeting triangles. (In the unfolded state, the central point is the center p of scaling.) Thus we obtain a rigid folding of a crease pattern with a single vertex p and one emanating edge per vertex of P, all with the same sign. But such a folding contradicts Lemma 16 . □

6 Existence of Triangulated Hyperbolic Paraboloid

In contrast to the classic hyperbolic paraboloid model, we show that triangulating each trapezoidal face and retriangulating the central ring permits folding:

Theorem 19 *The two mountain-valley patterns in Figure 4, with mountains and valleys matching the hyperbolic paraboloid of Figure 1(a), have proper foldings, uniquely determined by the fold angle*

θ of the central diagonal, that exist at least for n = 100 and θ ∈ {2°, 4°, 6°, ..., 178°} for the alternating asymmetric triangulation, and at least for n and θ shown in Table 1 for the asymmetric triangulation. For each θ ∈ {2°, 4°, ..., 178°}, the asymmetric triangulation has no proper folding for n larger than the limit values shown in Table 1.

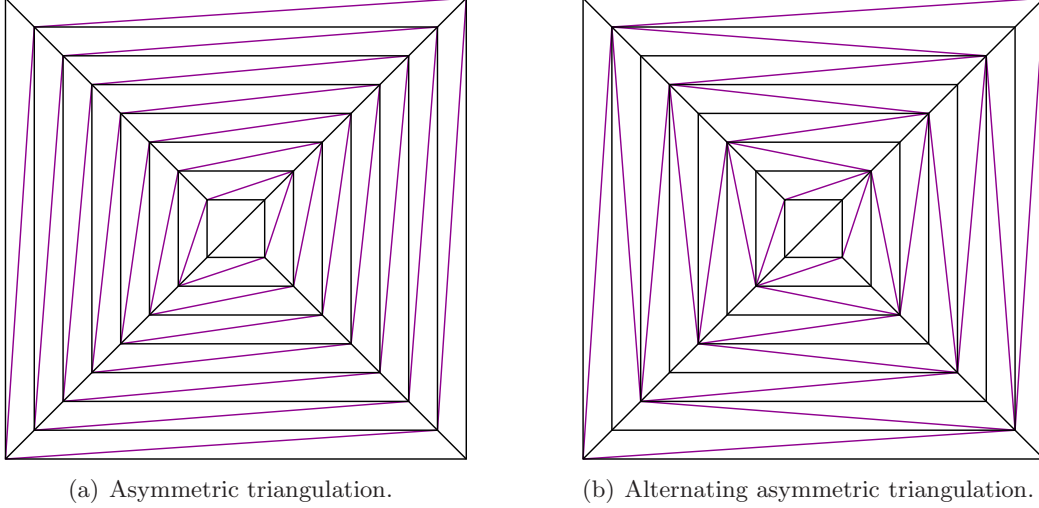(a) Asymmetric triangulation.   (b) Alternating asymmetric triangulation.

Figure 4: Two foldable triangulations of the hyperbolic paraboloid crease pattern (less one diagonal in the center).

θ	2°	4°	6°	8°	10°	12°	14°	16°	18°	20°	22°	24°	26°	28°	30°	32°
n	133	67	45	33	27	23	19	17	15	13	13	11	11	9	9	9

θ	34°	36°	38°	40°	42°	44°	46°	48°	50°	$\cdots$	72°	74°	76°	$\cdots$	176°	178°
n	9	7	7	7	7	7	7	5	5	$\cdots$	5	3	3	$\cdots$	3	3

Table 1: The largest n for which the asymmetric triangulation has a proper folding, for each $\theta \in \{2°, 4°, ..., 178°\}$. (By contrast, the alternating asymmetric triangulation has a proper folding for $n = 100$ for all such θ.) Interestingly, for θ not too large, $n \cdot \theta$ is roughly 270°.

Proof: The proof is by construction: we give a construction which implies uniqueness, and then use the resulting algorithm to construct the explicit 3D geometry using interval arithmetic and a computer program.

To get started, we are given the fold angle θ between the two triangles of the central square. By fixing one of these triangles in a canonical position, we obtain the coordinates of the central square's vertices by a simple rotation.

We claim that all other vertices are then determined by a sequence of intersection-of-three-spheres computations from the inside out. In the asymmetric triangulation of Figure 4(a), the lower-left and upper-right corners of each square have three known (creased) distances to three vertices from the previous square. Here we use Theorem 10 which guarantees that the creases remain straight and thus their endpoints have known distance. Thus we can compute these vertices as the intersections of three spheres with known centers and radii. Afterward, the lower-right and upper-left corners of the same square have three known (creased) distances to three known vertices,

11

one from the previous square and two from the current square. Thus we can compute these vertices also as the intersection of three spheres. In the alternating asymmetric triangulation of Figure 4(a), half of the squares behave the same, and the other half compute their corners in the opposite order (first lower-right and upper-left, then lower-left and upper-right).

The intersection of three generic spheres is zero-dimensional, but in general may not exist and may not be unique. Specifically, the intersection of two distinct spheres is either a circle, a point, or nothing; the further intersection with another sphere whose center is not collinear with the first two spheres' centers is either two points, one point, or nothing. When there are two solutions, however, they are reflections of each other through the plane containing the three sphere centers. (The circle of intersection of the first two spheres is centered at a point in this plane, and thus the two intersection points are equidistant from the plane.)

For the hyperbolic paraboloid, we can use the mountain-valley assignment (from Figure 1(a)) to uniquely determine which intersection to choose. In the first intersection of three spheres, one solution would make two square creases mountains (when the solution is below the plane) and the other solution would make those creases valleys. Thus we choose whichever is appropriate for the alternation. In the second intersection of three spheres, one solution would make a diagonal crease mountain, and the other solution would make that crease valley. Again we choose whichever is appropriate for the alternation. Therefore the folding is uniquely determined by θ and by the mountain-valley assignment of the original hyperbolic paraboloid creases.

This construction immediately suggests an algorithm to construct the proper folding. The coordinates of intersection of three spheres can be written as a radical expression in the center coordinates and radii (using addition, subtraction, multiplication, division, and square roots). See [Wik08] for one derivation; Mathematica's fully expanded solution for the general case (computed with `Solve`) uses over 150,000 leaf expressions (constant factors and variable occurrences). Thus, if the coordinates of the central square can be represented by radical expressions (e.g., θ is a multiple of 15°), then all coordinates in the proper folding can be so represented. Unfortunately, we found this purely algebraic approach to be computationally infeasible beyond the second square; the expressions immediately become too unwieldy to manipulate (barring some unknown simplification which Mathematica could not find).

Therefore we opt to approximate the solution, while still guaranteeing that an exact solution exists, via *interval arithmetic* [Hay03, MKC09, AH83]. The idea is to represent every coordinate x as an interval $[x_L, x_R]$ of possible values, and use conservative estimates in every arithmetic operation and square-root computation to guarantee that the answer is in the computed interval. For example, $[a, b] + [c, d] = [a + c, b + d]$ and $[a, b] \cdot [c, d] = [\min\{a \cdot c, a \cdot d, b \cdot c, b \cdot d\}, \max\{a \cdot c, a \cdot d, b \cdot c, b \cdot d\}]$, while $\sqrt{[a, b]}$ requires a careful implementation of a square-root approximation algorithm such as Newton's Method. The key exception is that $\sqrt{[a, b]}$ is undefined when $a < 0$. A negative square root is the only way that the intersection of three spheres, and thus the folding, can fail to exist. If we succeed in computing an approximate folding using interval arithmetic without attempting to take the square root of a partially negative interval, then an exact folding must exist. Once constructed, we need only check that the folding does not intersect itself (i.e., forms an embedding).

We have implemented this interval-arithmetic construction in Mathematica; refer to Appendix A. Using sufficiently many (between 1,024 and 2,048) digits of precision in the interval computations, the computation succeeds for the claimed ranges of n and θ for both triangulations. Table 2 shows how the required precision grows with n (roughly linearly), for a few different instances. Figure 5 shows some of the computed structures (whose intervals are much smaller than the drawn line thickness). The folding construction produces an answer for the asymmetric triangulation even for $n = 100$ and $\theta \in \{2°, 4°, \ldots, 178°\}$, but the folding self-intersects for n larger than the limit values

shown in Table 1. □

digits of precision	16	32	64	128	256	512	1024	2048
n for $\theta = 1°$	3	6	12	22	41	76	≥ 100	
n for $\theta = 1°$ alt.	3	6	12	24	43	79	≥ 100	
n for $\theta = 45°$ alt.	3	5	10	18	32	58	≥ 100	
n for $\theta = 76°$ alt.	2	5	9	16	29	53	95	≥ 100

Table 2: Number n of triangulated rings that can be successfully constructed using various precisions (measured in digits) of interval arithmetic.

We conjecture that this theorem holds for all n and all $\theta < 180°$ for the alternating asymmetric triangulation, but lack an appropriately general proof technique. If the construction indeed works for all θ in some interval $[0, \Theta)$, then we would also obtain a continuous folding motion.

(a) Asymmetric triangulation, $\theta = 8°$, $n = 16$.

(b) Alternating asymmetric triangulation, $\theta = 30°$, $n = 16$.
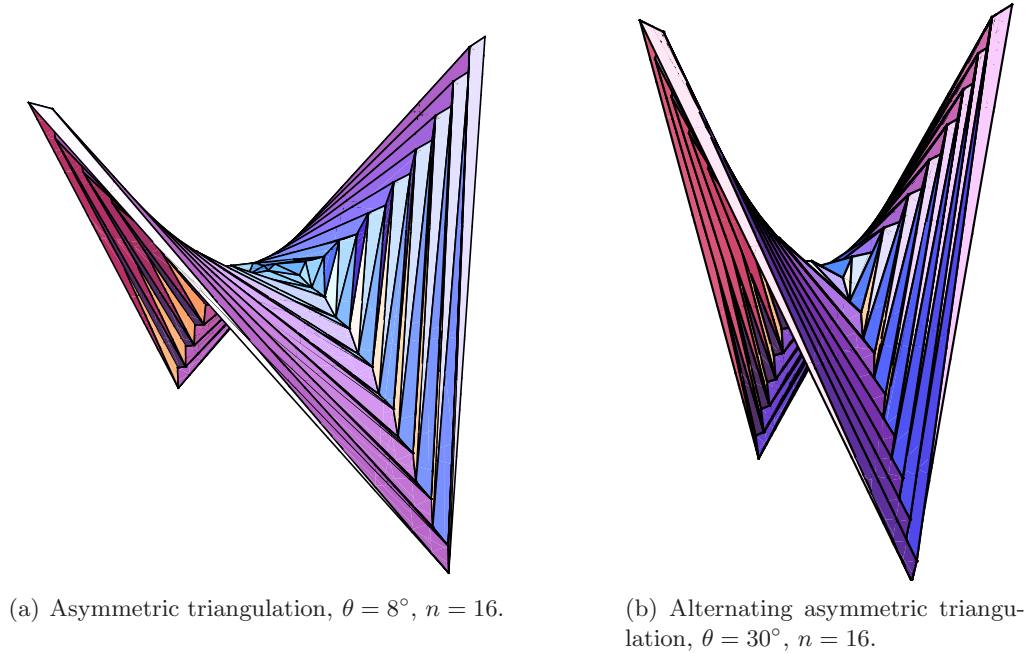
Figure 5: Proper foldings of triangulated hyperbolic paraboloids.

Interestingly, the diagonal cross-sections of these structures seem to approach parabolic in the limit. Figure 6 shows the $x = y \geq 0$ cross-section of the example from Figure 5(b), extended out to $n = 100$. The parabolic fit we use for each parity class is the unique quadratic polynomial passing through the three points in the parity class farthest from the center. The resulting error near the center is significant, but still much smaller than the diagonal crease length, $\sqrt{2}$. Least-square fits reduce this error but do not illustrate the limiting behavior.
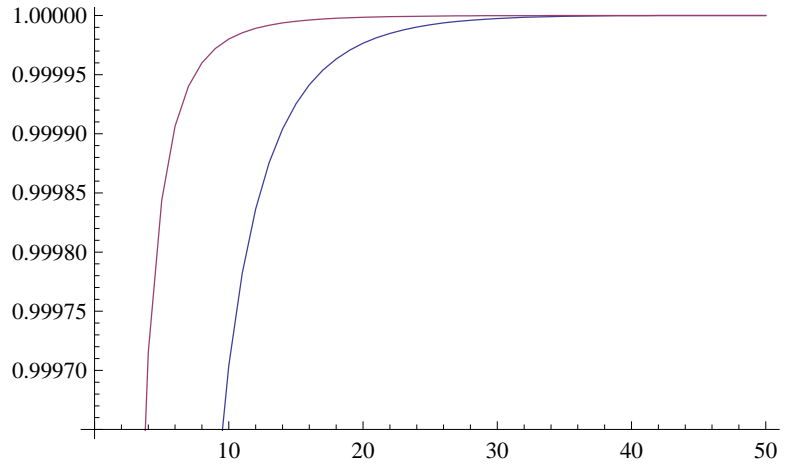
7 Smooth Hyperbolic Paraboloid

Given a smooth plane curve Γ and an embedding of Γ in space as a smooth space curve γ, previous work [FT99] has studied the problem of folding a strip of paper so that a crease in the form of Γ in

13
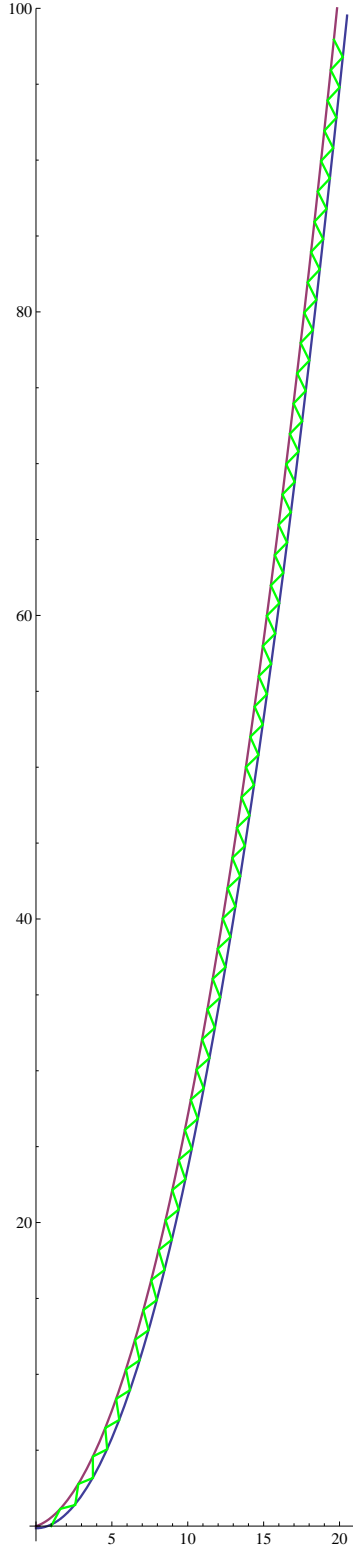
(a) Actual zig-zag and parabolic fits.
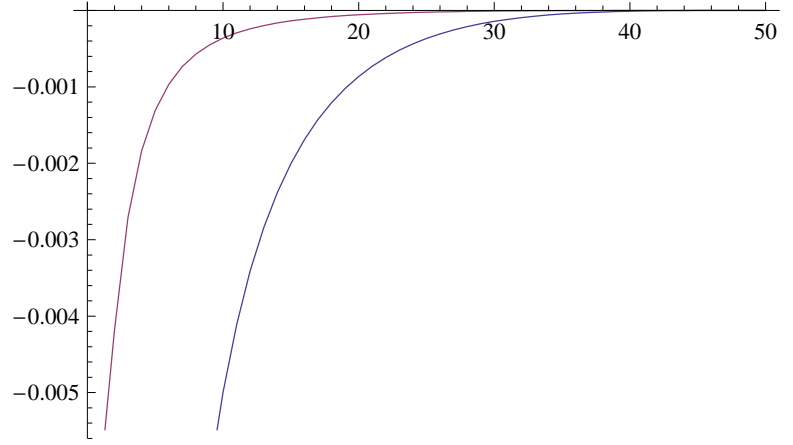
(b) Absolute difference: fit minus actual.

(c) Relative difference: fit over actual.

Figure 6: Planar cross-section of alternating asymmetric triangulation, $\theta = 30°$, $n = 100$, with parabolic fits of each parity class based on the last three vertices.

the plane follows the space curve γ when folded. The main theorem from this work is that such a folding always exists, at least for a sufficiently narrow strip about Γ, under the condition that the curvature of γ be everywhere strictly greater than that of Γ.

Further, with some differential geometry described in [FT99], it is possible to write down exactly how the strip folds in space; there are always exactly two possible choices, and additionally two ways to fold the strip so that Γ lies along γ but remains uncreased.

Based on some preliminary work using these techniques, we conjecture that the circular pleat indeed folds, and that so too does any similar crease pattern consisting of a concentric series of convex smooth curves. Unfortunately a proof remains elusive. Such a proof would be the first proof to our knowledge of the existence of any curved-crease origami model, beyond the local neighborhood of a single crease.

Acknowledgments

References

[Adl04]   Esther Dora Adler. *"A New Unity!" The Art and Pedagogy of Josef Albers*. PhD thesis, University of Maryland, 2004.

[AH83]   Götz Alefeld and Jürgen Herzberger. *Introduction to Interval Computations*. Academic Press, 1983.

[DD08]   Erik D. Demaine and Martin L. Demaine. History of curved origami sculpture. http://erikdemaine.org/curved/history/, 2008.

[DDL99]   Erik D. Demaine, Martin L. Demaine, and Anna Lubiw. Polyhedral sculptures with hyperbolic paraboloids. In *Proceedings of the 2nd Annual Conference of BRIDGES: Mathematical Connections in Art, Music, and Science (BRIDGES'99)*, pages 91–100, Winfield, Kansas, July 30–August 1 1999.

[DO02]   Melody Donoso and Joseph O'Rourke. Nonorthogonal polyhedra built from rectangles. arXiv:cs/0110059v2 [cs.CG], May 2002. http://www.arXiv.org/abs/cs.CG/0110059. Abstract in *Proceedings of the 14th Canadian Conference on Computational Geometry*, Lethbridge, Canada, August 2002, pages 101–104.

[FT99]   Dmitry Fuchs and Serge Tabachnikov. More on paperfolding. *American Mathematical Monthly*, 106(1):27–35, 1999.

[Gau02]   Carl Friedrich Gauss. *General Investigations of Curved Surfaces*. Princeton University Library, 1902. Translated by J. C. Morehead and A. M. Hiltebeitel from 1827 original. Republished by Dover, 2005.

[Hal85]   George Bruce Halsted. *Elements of Geometry*. John Wiley & Sons, 1885. http://books.google.com/books?id=HCdoFvAcHyIC.

[Hay03]   Brian Hayes. A lucid interval. *American Scientist*, 91(6):484–488, November–December 2003.

[KDD08]   Duks Koschitz, Erik D. Demaine, and Martin L. Demaine. Curved crease origami. In *Abstracts from Advances in Architectural Geometry (AAG 2008)*, pages 29–32, Vienna, Austria, September 13–16 2008.

[MKC09]   Ramon E. Moore, R. Baker Kearfott, and Michael J. Cloud. *Introduction to Interval Analysis*. SIAM Press, 2009.

[Spi79]   Michael Spivak. *A Comprehensive Introduction to Differential Geometry*. Publish or Perish, second edition, 1979.

[Wer05]   Margaret Wertheim. Origami as the shape of things to come. *The New York Times*, February 15 2005. http://www.nytimes.com/2005/02/15/science/15origami.html.

[Wik08]   Wikipedia. Trilateration. http://en.wikipedia.org/wiki/Trilateration, 2008.

[Win69]   Hans M. Wingler. *Bauhaus: Weimar, Dessau, Berlin, Chicago*. MIT Press, 1969.

A   Mathematica Construction of Triangulated Hyperbolic Paraboloid

```
SW = 1; SE = 2; NE = 3; NW = 4;
next[d_] := 1 + Mod[d, 4];
prev[d_] := 1 + Mod[d + 2, 4];
square[i_] := {{-i, -i}, {i, -i}, {i, i}, {-i, i}};
side[i_] := 2 i;
diagonal[i_] := Sqrt[2] side[i];
diagpiece[i_] := Sqrt[2];
cross[i_] := Sqrt[(i - (i - 1))^2 + (i + (i - 1))^2];
n = 100;
bigside := side[n];
bigdiagonal := diagonal[n];
trapezoid[i_, d_] :=
  square[i][[{d, next[d]}]] ~Join~ square[i - 1][[{next[d], d}]];

(* Note: \[Theta] is half the fold angle. *)
algebraicmiddle := {
  {-1, -1, 0}, {-Cos[\[Theta]], Cos[\[Theta]], Sqrt[2] Sin[\[Theta]]},
  {1, 1, 0}, {Cos[\[Theta]], -Cos[\[Theta]], Sqrt[2] Sin[\[Theta]]}};
precision = 1024;
middle := Map[Interval[N[#, precision]] &, algebraicmiddle, {2}];

orientation[a_, b_, c_, d_] :=
  Sign[Det[Append[#, 1] & /@ {a, b, c, d}]];
pickorientation[choices_, a_, b_, c_, pos_] :=
  Module[
    {select = Select[choices,
                      If[pos, orientation[a, b, c, #] >= 0 &,
                              orientation[a, b, c, #] <= 0 &]]},
    If[Length[select] > 1,
      Print["Warning: Multiple choices in pickorientation..."]];
    If[Length[select] > 0, select[[1]],
```

```
           Print["Couldn't find mountain/valley choice"]]];
triangles[1] := {triangulated[[1, {1, 2, 3}]], triangulated[[1, {3, 4, 1}]]};

threespheres =
  Solve[{SquaredEuclideanDistance[{x1, y1, z1}, {x, y, z}] == d1^2,
    SquaredEuclideanDistance[{x2, y2, z2}, {x, y, z}] == d2^2,
    SquaredEuclideanDistance[{x3, y3, z3}, {x, y, z}] == d3^2}, {x, y, z}];
solvethreespheres[{X1_, Y1_, Z1_}, D1_, {X2_, Y2_, Z2_},
  D2_, {X3_, Y3_, Z3_}, D3_] :=
  threespheres /. {x1 -> X1, y1 -> Y1, z1 -> Z1, x2 -> X2, y2 -> Y2,
    z2 -> Z2, x3 -> X3, y3 -> Y3, z3 -> Z3, d1 -> D1, d2 -> D2, d3 -> D3};

checklengths := Module[{i, j, t, tri, error, maxerror, who},
  maxerror = 0;
  who = "I did not see any error!";
  For[i = 1, i <= Length[triangulated], i++,
    For[t = 1, t <= Length[triangles[i]], t++,
      tri = triangles[i][[t]];
      For[j = 1, j <= 3, j++,
        error =
          Min[Abs[EuclideanDistance[tri[[j]], tri[[Mod[j, 3] + 1]]] - #] & /@
              If[i == 1, {side[i], 2 diagpiece[i]},
                        {side[i], side[i - 1], cross[i], diagpiece[i]}]];
        If[error >= maxerror,
          who = {"i=", i, " triangle ", t, " edge ", j, "-",
            Mod[j, 3] + 1, " has error ", error, " = ", N[error], ": ",
            EuclideanDistance[tri[[j]], tri[[Mod[j, 3] + 1]]],
            " vs. ", {side[i], side[i - 1], cross[i], diagpiece[i]}};
          maxerror = error]]]];
  Print @@ who];

(* Collision detection *)
stL = Solve[{(1 - L) ax + L bx ==
        px + s (qx - px) + t (rx - px), (1 - L) ay + L by ==
        py + s (qy - py) + t (ry - py), (1 - L) az + L bz ==
        pz + s (qz - pz) + t (rz - pz)}, {s, t, L}][[1]];
pierces[seg_, tri_] := Module[{parms},
  Check[Quiet[
    parms = stL /. {ax -> seg[[1]][[1]], ay -> seg[[1]][[2]],
      az -> seg[[1]][[3]], bx -> seg[[2]][[1]], by -> seg[[2]][[2]],
      bz -> seg[[2]][[3]], px -> tri[[1]][[1]],
      py -> tri[[1]][[2]], pz -> tri[[1]][[3]], qx -> tri[[2]][[1]],
      qy -> tri[[2]][[2]], qz -> tri[[2]][[3]],
      rx -> tri[[3]][[1]], ry -> tri[[3]][[2]],
      rz -> tri[[3]][[3]]};
    spt = (s + t) /. parms; LL = L /. parms;
    Return[(s > 0 && t > 0 && s + t < 1 && 0 < L < 1) /.
      parms], {Power::"infy", \[Infinity]::"indet"}],
   Return[False], {Power::"infy", \[Infinity]::"indet"}]];
checkcollision := Module[{i, j, t, t2, tri, seg},
  For[i = 1, i <= Length[triangulated] - 1, i++,
    PrintTemporary["Ring ", i, " vs. ", i + 1];
    For[t = 1, t <= Length[triangles[i]], t++,
```

```
        tri = triangles[i][[t]];
        For[t2 = 1, t2 <= Length[triangles[i + 1]], t2++,
          For[j = 1, j <= 3, j++,
            seg = triangles[i + 1][[t2]][[{j, Mod[j, 3] + 1}]];
            If[Length[Intersection[seg, tri]] > 0, Continue[]];
            If[pierces[seg, tri],
              Print["COLLISION! ", i, ",", t, " vs. ", i + 1, ",", t2, ",", j];
              Return[{seg, tri}]]]]]]];
  Print["No collision."]];

adaptiveprecisiontest[mint_, maxt_, tstep_: 1, minprecision_: 8, maxprecision_: 65536] :=
  Module[{t},
    precision = minprecision;
    Print["n: ", n];
    For[t = mint, t <= maxt, t = t + tstep,
      Print[t, " degrees:"];
      \[Theta] = t \[Pi]/180;
      For[True, precision <= maxprecision, precision = 2 precision,
        Print["precision: ", precision];
        If[computetriangulated == n,
          Print["Required precision for ", t, " degrees:", precision];
          checklengths; checkcollision; Break[]]]]];

Print["ALTERNATING ASYMMETRIC TRIANGULATED FOLDING"];

oddoutset [i_, d_, last_] :=
  pickorientation[{x, y, z} /. # & /@
    solvethreespheres[last[[d]], diagpiece[i], last[[next[d]]],
      cross[i], last[[prev[d]]], cross[i]],
    last[[prev[d]]], last[[d]], last[[next[d]]], OddQ[i]];
evenoutset[i_, d_, last_, odds_] :=
  pickorientation[{x, y, z} /. # & /@
    solvethreespheres[last[[d]], diagpiece[i], odds[[next[d]]],
      side[i], odds[[prev[d]]], side[i]],
    odds[[prev[d]]], last[[d]], odds[[next[d]]], OddQ[i]];
computetriangulated := Module[{i, odds},
  triangulated = {middle};
  For[i = 2, i <= n, i++,
    If[OddQ[i],
      last = RotateRight[triangulated[[-1]]],
      last = triangulated[[-1]]];
    odds = Table[If[OddQ[d], oddoutset[i, d, last]], {d, 1, 4}];
    Print["Round ", i, " odds done"];
    If[Count[odds, Null] > 2, Break[]];
    both =
      Table[If[OddQ[d], odds[[d]], evenoutset[i, d, last, odds]], {d, 1, 4}];
    If[OddQ[i],
      AppendTo[triangulated, RotateLeft[both]],
      AppendTo[triangulated, both]];
    Print["Round ", i, " evens done"];
    If[Count[triangulated[[-1]], Null] > 0, Break[]]];
  Print[i - 1, " rounds complete"];
  i-1];
```

```
triangles[i_] :=
  Flatten[Table[
    If[OddQ[d] == EvenQ[i],
      {{triangulated[[i, d]], triangulated[[i - 1, d]],
        triangulated[[i - 1, prev[d]]]},
       {triangulated[[i, d]], triangulated[[i - 1, d]],
        triangulated[[i - 1, next[d]]]}},
      {{triangulated[[i, d]], triangulated[[i - 1, d]],
        triangulated[[i, prev[d]]]},
       {triangulated[[i, d]], triangulated[[i - 1, d]],
        triangulated[[i, next[d]]]}}], {d, 1, 4}], 1];

adaptiveprecisiontest[1, 90];

Print["ASYMMETRIC TRIANGULATED FOLDING"];

computetriangulated := Module[{i, odds},
  triangulated = {middle};
  For[i = 2, i <= n, i++,
    odds = Table[If[OddQ[d], oddoutset[i, d, triangulated[[-1]]]], {d, 1, 4}];
    Print["Round ", i, " odds done!"];
    If[Count[odds, Null] > 2, Break[]];
    AppendTo[triangulated,
      Table[If[OddQ[d], odds[[d]],
        evenoutset[i, d, triangulated[[-1]], odds]], {d, 1, 4}]];
    Print["Round ", i, " evens done"];
    If[Count[triangulated[[-1]], Null] > 0, Break[]]];
  Print[i - 1, " rounds complete"];
  i-1];
triangles[i_] :=
  Flatten[Table[
    If[OddQ[d],
      {{triangulated[[i, d]], triangulated[[i - 1, d]],
        triangulated[[i - 1, prev[d]]]},
       {triangulated[[i, d]], triangulated[[i - 1, d]],
        triangulated[[i - 1, next[d]]]}},
      {{triangulated[[i, d]], triangulated[[i - 1, d]],
        triangulated[[i, prev[d]]]},
       {triangulated[[i, d]], triangulated[[i - 1, d]],
        triangulated[[i, next[d]]]}}], {d, 1, 4}], 1]

adaptiveprecisiontest[1, 90];
```